Gate control of spin dynamics in III-V semiconductor quantum dots

Rogerio de Sousa and S. Das Sarma
Condensed Matter Theory Center, Department of Physics, University of Maryland, College Park, Maryland 20742-4111, USA
(Received 23 April 2003; revised manuscript received 14 August 2003; published 27 October 2003)

We show that the g factor and the spin-flip time T_1 of a heterojunction quantum dot is very sensitive to the band-bending interface electric field even in the absence of wave-function penetration into the barrier. When this electric field is of the order of 10^5 V/cm, g and T_1 show high sensitivity to dot radius and magnetic field arising from the interplay between Rashba and Dresselhaus spin-orbit interactions. This result opens new possibilities for the design of a quantum dot spin quantum computer, where g factor and T_1 can be engineered by manipulating the spin-orbit coupling through external gates.

DOI: 10.1103/PhysRevB.68.155330 PACS number(s): 73.21.La, 03.67.Lx, 71.70.Ej, 85.35.Be

Understanding and controlling the behavior of spins in semiconductor heterostructures may lead to a whole new class of devices,[1,2] ranging from spin-polarized p-n junctions[3] to a quantum dot spin quantum computer.[4] Electrical control over spin-orbit coupling parameters in a quantum well has long been suggested as an effective means to manipulate spin,[5] and was recently experimentally demonstrated in InAs heterostructures.[6] This was possible because the Rashba[7,8] and the Dresselhaus[9] spin-orbit interactions are sensitive to the electric field providing vertical confinement to a two-dimensional electron gas (2DEG), which is approximately proportional to the 2DEG density and can be controlled through a gate voltage. When additional gates provide lateral confinement, a single electron can be trapped in a quantum dot (QD),[10] whose orbital states in an external magnetic field perpendicular to the 2DEG are the well-known Fock-Darwin states.[11] Here we consider the effect of Rashba and Dresselhaus spin-orbit interactions in the spin-doublet ground state of a Fock-Darwin QD. Using an effective-mass approximation and exact diagonalization of a Fock-Darwin subspace we show that the ground-state g factor and spontaneous phonon emission rate $1/T_1$ (due to the spin-orbit admixture mechanism)[12] can be substantially manipulated by varying the heterojunction electric field in the range of 10^5–10^6 V/cm (corresponding to 2DEG density of the order of 10^{12}–10^{13} cm^{-2}).

Recently, electrical control over GaAs quantum well g factor has been achieved by forcing the electron wave function to overlap with the AlGaAs barrier.[13,14] Here we intentionally neglect barrier penetration, to show that overlap with a different material *is not a necessary condition to achieve substantial electrical control over quantum dot g* factor. Moreover, by avoiding barrier penetration one can suppress an additional spin-lattice relaxation mechanism due to interface motion.[15] These results open new possibilities in the design of a quantum dot quantum computer: for example, spin qubits can be brought in and out of resonance to a global spin resonance field by gate control of their g factor;[16] a speed up in quantum computer initialization (setting up all spins for example) can be achieved by decreasing the spin-flip time T_1 with a gate voltage.

The Hamiltonian for a single electron bound to a heterojunction quantum dot can be divided into five parts,

$$\mathcal{H}=\mathcal{H}_0+\mathcal{H}_z+\mathcal{H}_R+\mathcal{H}_{D1}+\mathcal{H}_{D2}. \tag{1}$$

The first contribution corresponds to a single 2D electron confined in the xy plane by a parabolic potential and subject to a magnetic field $\mathbf{B}$,

$$\mathcal{H}_0=\frac{\mathbf{P}^2}{2m^*}+\frac{1}{2}m^*\omega_0^2r^2+\frac{1}{2}g_0\mu_B\sigma_zB, \tag{2}$$

where the kinetic momentum $\mathbf{P}=\mathbf{p}+e/c\mathbf{A}$ is written with the canonical momentum $\mathbf{p}=-i\hbar(\partial_x,\partial_y,0)$ and vector potential $\mathbf{A}=B/2(-y,x,0)$ confined to the 2D plane. Here e is the electron charge, c is the velocity of light, m^* is the conduction-band edge effective mass, ω_0 is the parabolic confining potential frequency, g_0 is the bulk g factor, μ_B is the Bohr magneton, and σ_z is the diagonal Pauli matrix. $\mathcal{H}_0$ is diagonal when written as a function of the Fock-Darwin number operators $n_\pm=a_\pm^\dagger a_\pm$,[11]

$$\mathcal{H}_0=\hbar\omega_+\left(n_++\frac{1}{2}\right)+\hbar\omega_-\left(n_-+\frac{1}{2}\right)+\frac{1}{2}g_0\mu_B\sigma_zB, \tag{3}$$

$$a_\pm^\dagger=\frac{1}{2\ell}(x\pm iy)-\frac{\ell}{2}(\partial_x\pm i\partial_y), \tag{4}$$

$$a_\pm=\frac{1}{2\ell}(x\mp iy)+\frac{\ell}{2}(\partial_x\mp i\partial_y). \tag{5}$$

Here $\omega_\pm=\Omega\pm\omega_c/2$, with $\Omega=\sqrt{\omega_0^2+\omega_c^2/4}$ and $\omega_c=eB/m^*c$ being the renormalized dot frequency and cyclotron frequency, respectively, with $\ell=\sqrt{\hbar/m^*\Omega}$ being the Fock-Darwin radius which sets the length scale for the eigenstates $|n_+n_-\sigma\rangle$ ($\sigma=\pm1$ represents the spin up/down states in the z direction). The second term in Hamiltonian (1) represents the quantum well confinement in the growth z direction, $\mathcal{H}_z=p_z^2/2m^*+V(z)$, where $V(z)$ is a triangular well, $V(z)=eEz$ for $z\geqslant0$ and $V(z)=\infty$ for $z<0$. A simple numerical calculation leads to the $\mathcal{H}_z$ ground state

$$\Psi_{0z}(z)=1.4261\kappa^{1/2}\mathrm{Ai}(\kappa z+\zeta_1), \tag{6}$$

where $\zeta_1=-2.3381$ is the first zero of the Airy function Ai, while the inverse length scale κ is set by

$$\kappa=(2m^*eE/\hbar^2)^{1/3}, \tag{7}$$

and the ground-state energy is $E_{0z}=-\zeta_1eE/\kappa$. In the discussion below we will make use of the average momentum

TABLE I. Parameters used in our calculations (Refs. 8,22).

Parameter		GaAs	GaSb	InAs	InSb
g_0		-0.44	-7.8	-15	-50.6
m^*/m_e		0.067	0.0412	0.0239	0.0136
α_R	[Å^2]	4.4	33	110	500
γ_c	[eV Å^3]	26	187	130	228
eh_{14}	[10^{-5} erg/cm]	2.34	1.5	0.54	0.75
s_L	[10^5 cm/s]	5.14	4.30	4.20	3.69
s_T	[10^5 cm/s]	3.03	2.49	2.35	2.29
ρ	[g/cm^3]	5.3176	5.6137	5.6670	5.7747

squared in the state (6), $\langle p_z^2\rangle = 0.7794(\hbar\kappa)^2$, and the average position $\langle z\rangle = 1.558\,7/\kappa$ (which is the thickness of the 2DEG). We now turn to the spin-orbit interactions, third to fifth terms in Eq. (1). A $\mathbf{k}\cdot\mathbf{p}$ band-structure calculation for zincblende materials[9] leads to the bulk conduction-band spin-orbit interaction

$$\mathcal{H}_{\rm Bulk} = \gamma_c/(2\hbar^3)\boldsymbol{\sigma}\cdot\tilde{\mathbf{P}}, \tag{8}$$

where $\tilde{P}_x = P_x(P_y^2 - P_z^2) + \text{H.c.}$, $\tilde{P}_y$ and $\tilde{P}_z$ can be obtained by cyclic permutations. Note that Eq. (8) is Hermitian and gauge invariant. The value of γ_c is determined by the band-structure parameters of the III-V semiconductors (Table I). By averaging Eq. (8) over the quantum well ground state [Eq. (6)] we get two spin-orbit terms, linear and cubic in momenta (here the quantum well growth direction is assumed to be [001]),[17]

$$\mathcal{H}_{\rm D1} = 0.7794\gamma_c\kappa^2/\hbar(-\sigma_x P_x + \sigma_y P_y), \tag{9}$$

$$\mathcal{H}_{\rm D2} = \gamma_c/\hbar^3(\sigma_x P_x P_y^2 - \sigma_y P_y P_x^2) + \text{H.c.} \tag{10}$$

The structural inversion asymmetry in $V(z)$ leads to the Rashba interaction[8]

$$\mathcal{H}_{\rm R} = \alpha_R eE/\hbar(\sigma_x P_y - \sigma_y P_x), \tag{11}$$

which for the triangular well considered here is directly proportional to E (α_R depends on band-structure parameters).[8] It is useful to condense $\mathcal{H}_{\rm R}$ and $\mathcal{H}_{\rm D1}$ in a single Hamiltonian written as a function of the Fock-Darwin operators,

$$\mathcal{H}_{\rm D1} + \mathcal{H}_{\rm R} = \hat{V}\sigma_+ + \hat{V}^\dagger\sigma_-, \tag{12}$$

$$\hat{V} = -\alpha_- a_-^\dagger + \alpha_+ a_+ + i\beta_- a_- - i\beta_+ a_+^\dagger, \tag{13}$$

with $\sigma_\pm = (\sigma_x \pm i\sigma_y)/2$ and spin-orbit energy scales defined as

$$\alpha_\pm = \alpha_R eE\xi_\pm, \tag{14}$$

$$\beta_\pm = 0.78\gamma_c\kappa^2\xi_\pm, \tag{15}$$

$$\xi_\pm = \frac{1}{\ell} \pm \frac{eB\ell}{2\hbar c}. \tag{16}$$

Therefore $\mathcal{H}_{\rm R}$ and $\mathcal{H}_{\rm D1}$ couples Fock-Darwin levels differing by one quantum number. The amount of spin up/down admixture in the ground state is given by the ratios $\alpha_\pm/\hbar\omega_0$, $\beta_\pm/\hbar\omega_0$, which at $B\approx 0$ are directly proportional to the dot radius $l_0 = \sqrt{\hbar/m^*\omega_0}$. Therefore larger dots will be more sensitive to spin-orbit coupling, at least within perturbation theory (see below). Moreover, the question whether Rashba or Dresselhaus dominates depends only on material parameters and electric field, since $\alpha_\pm/\beta_\pm = \alpha_R/\gamma_c(\hbar^2/m^*)^{2/3}(eE)^{1/3}$. If the electric field ranges from 10^4–10^6 V/cm this ratio equals 0.1–0.7 for GaAs, 0.2–1.0 for GaSb, 1.5–6.8 for InAs, and 5.6–26 for InSb. Therefore for III-V semiconductor quantum dots it is important to consider the interplay between Rashba and Dresselhaus spin-orbit interactions. High-electric-field GaSb heterojunctions might realize the condition $\alpha_\pm = \beta_\pm$, leading to an interesting simplification of Eq. (12), which becomes proportional to $(\sigma_x + \sigma_y)$.[18] However this symmetry is broken by Eq. (2), which contains a magnetic field pointing in the [001] direction. Hence it will have no consequences here [the highly symmetric case of $\mathbf{B}\|$ [110] and $\alpha_\pm = \beta_\pm$ leads to QD g factor exactly equal to the bulk value g_0, with no spin-lattice relaxation, as long as the cubic spin-orbit interaction Eq. (10) is neglected].

We now turn to the cubic spin-orbit term [Eq. (10)],

$$\begin{aligned}\mathcal{H}_{\rm D2} = -i\sigma_+\Big[&\lambda_1 a_-^{\dagger 2}a_+ + \lambda_2 a_+^{\dagger 2}a_- + \lambda_4 a_- n_- - \lambda_3 a_+^\dagger(n_+ + 1) \\ &+ \frac{\lambda_2}{3}a_-(2n_+ + 1) - \frac{\lambda_1}{3}a_+^\dagger(2n_- + 1) + \frac{\lambda_2}{3}a_+^{\dagger 2}a_-^\dagger \\ &- \frac{\lambda_1}{3}a_+ a_-^2 - \lambda_4 a_-^{\dagger 3} + \lambda_3 a_+^3\Big] + \text{H.c.},\end{aligned} \tag{17}$$

with $\lambda_1 = 3/4\gamma_c\xi_+\xi_-^2$, $\lambda_2 = 3/4\gamma_c\xi_-\xi_+^2$, $\lambda_3 = 1/4\gamma_c\xi_+^3$, $\lambda_4 = 1/4\gamma_c\xi_-^3$. $\mathcal{H}_{\rm D2}$ is often neglected,[17] a well-justified approximation for heterojunctions with a small Fermi wave vector ($\mathcal{H}_{\rm D2}$ was considered recently in a different context).[19] However, we will show that $\mathcal{H}_{\rm D2}$ leads to two interesting effects for small few electron quantum dots. The first term in Eq. (17) with its Hermitian conjugate couples the state $|n_+ n_- \sigma\rangle$ with $|n_+ + \sigma, n_- - 2\sigma, -\sigma\rangle$, which are degenerate at $\omega_c \approx \omega_0/\sqrt{2}$ (the exact location of the anticrossing depends on Zeeman splitting). The magnitude of the anticrossing is given by

$$\Delta E \approx \frac{2^{3/4}}{\sqrt{3}}\frac{\gamma_c}{l_0^3}\sqrt{n_+(n_- + 1)(n_- + 2)}. \tag{18}$$

For a GaAs dot with $l_0 = 10$ nm, $\Delta E \sim 0.1$ meV, while for GaSb, InAs, and InSb it can reach 1 meV. Note, however, that this anticrossing appears only for $n_+ + n_- > 1$. It may have interesting consequences for spin dependent transport through a few electron QD. The third to sixth terms in Eq. (17) are linear in $a_\pm$, $a_\pm^\dagger$ leading to an enhancement of the spin-orbit effect [Eq. (13)]. This affects our g factor and T_1 calculations by as much as a factor of 2, when $l_0 \lesssim 10$ nm.

Our QD ground-state g factor is defined by $g = (E_2 - E_1)/(\mu_B B)$, E_1 and E_2 being the ground and first excited states including spin. Considering Eq. (12) as a second-order perturbation to Eq. (2) with B field in the [001] direction we get

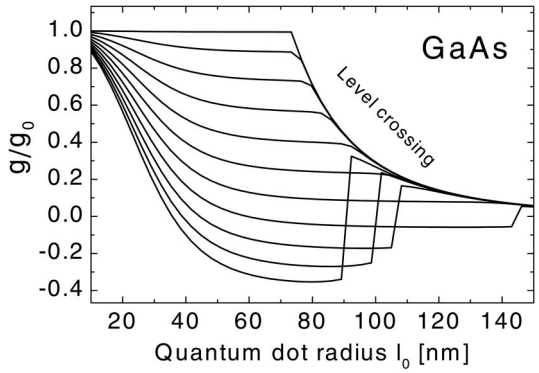

FIG. 1. Quantum dot g factor divided by the bulk g factor as a function of the dot radius $l_0=\sqrt{\hbar/m^*\omega_0}$ for a GaAs heterojunction. Each curve corresponds to a different electric field: From top to bottom, $E=10^4$, 1,2, . . . ,10×10^5. The magnetic field applied in the growth [100] direction is assumed to be 1 T. At large l_0 the two lowest-energy states have same spin, hence the level crossing. The results for GaSb are similar, except that the level crossing occurs for smaller l_0.

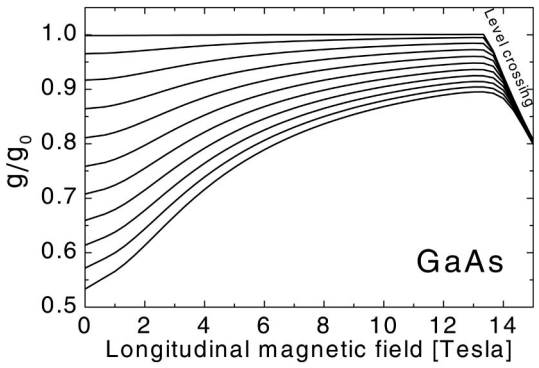

FIG. 2. Quantum dot g factor as a function of the magnetic field B for a GaAs heterojunction. The electric fields are the same as in Fig. 1. Dot radius is $l_0=20$ nm. At large B a similar level crossing as in Fig. 1 takes place.

$$g\approx g_0+2\frac{m_e m^*}{\hbar^4}[0.6\gamma_c^2\kappa^4(1-\delta)$$

$$-\alpha_R^2 e^2E^2(1+\delta)]\ell_0^2-\frac{1}{2}\frac{m_e m^{*3}}{\hbar^6}$$

$$\times\{0.6\gamma_c^2\kappa^4(1-\delta+\delta^2+\delta^3)-\alpha_R^2e^2E^2(1+\delta+\delta^2-\delta^3)\}$$

$$\times\omega_c^2\ell_0^6+\mathcal{O}(\omega_c/\omega_0)^4. \quad (19)$$

Here, $\delta=g_0m^*/m_e$, this expression being valid up to second order in ω_c/ω_0 and the spin-orbit admixtures. Clearly one sees that g factor displays a rich behavior as a function of QD radius and electric field. In particular, $g-g_0$ will be positive and proportional to $E^{4/3}$ if the Dresselhaus spin-orbit interaction is dominating (GaAs and GaSb), but negative and proportional to E^2 when Rashba dominates (InAs, InSb). In addition these effects increase with increasing dot radius l_0, and there is a B^2 dependence at higher magnetic fields.

We study the g-factor behavior at high electric and magnetic fields, and large dot radius by resorting to exact diagonalization of the full Hamiltonian [Eq. (1)] (similar calculations for Landau levels in a quantum well are available).[20] Our basis consists of nine Fock-Darwin shells ($n_+ + n_- \leq 8$), which together with spin leads to a 90×90 matrix for the Hamiltonian. Figs. 1 and 2 show results for GaAs, Figs. 3 and 4 for InAs. GaSb shows very similar behavior to GaAs, while InSb is similar to InAs. The differences between the two sets of materials is attributed to Dresselhaus spin-orbit interaction dominating in Figs. 1 and 2, but Rashba dominating in Figs. 3 and 4 (the Rashba interaction appears to be dominant in SiGe heterostructures, therefore g-factor behavior should be similar to the InAs case considered here, except that α_R is three orders of magnitude smaller and $g_0\approx2$; hence the effects considered here should be quite small for Si heterojunctions: we estimate $g-g_0\sim-10^{-3}$ for $E\sim10^5$ V/cm).[21] Our result suggests g factor can be controlled by a gate voltage (that either changes the longitudinal electric field E or the lateral confinement l_0) *as long as* $E\sim10^5$ V/cm. An important feature of Figs. 1–4 is that a level crossing takes place for large enough l_0 and B. In this regime the two lowest energy states of the QD are approximate Landau levels with the same spin, leading to extremely fast phonon emission rates (see below). Hence a QD quantum computer should operate away from this level crossing, which is actually a smooth anticrossing for InAs (see Figs. 3 and 4). Note that Figs. 1–4 plot the ratio of QD to bulk g factor (g/g_0), therefore the corresponding deviation in QD Zeeman energy from the bulk value will be rather appreciable for GaSb, InAs, and InSb since these materials have $g_0\sim-10$ (Table I).

We now turn to calculations of the transition rate between the two lowest-energy states due to spontaneous phonon emission. The electron-piezophonon interaction[12]

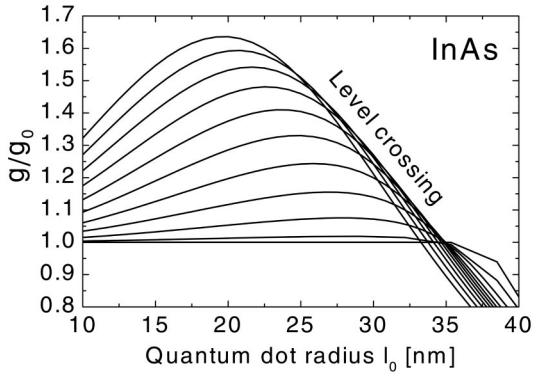

FIG. 3. Ratio between dot g factor and bulk g factor as a function of the dot radius l_0 for an InAs heterojunction. Each curve corresponds to an electric field, from bottom to top, $E=10^4$, 1,2, . . . ,10×10^5. The magnetic field applied in the growth [100] direction is assumed to be 1 T. Note the qualitative difference with respect to Fig. 1. Here Rashba interaction dominates the g factor, while in Fig. 1 Dresselhaus dominates. The results for InSb are similar.

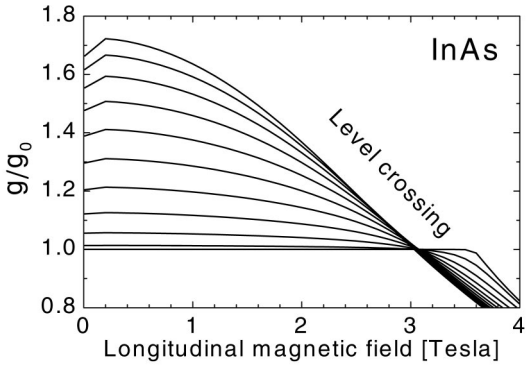

FIG. 4. g/g_0 as a function of magnetic field for an InAs heterojunction quantum dot with $l_0=20$ nm. Electric fields are the same as in Fig. 3. The results for InSb are similar.

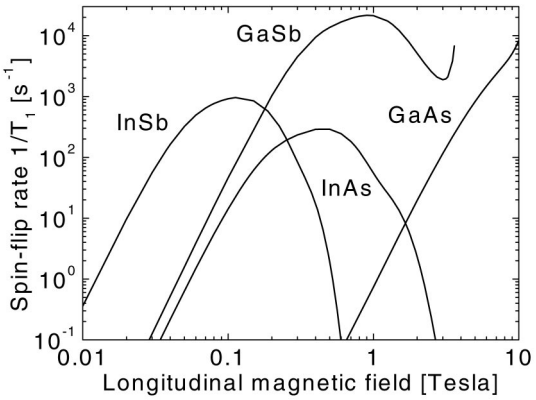

FIG. 5. Spin-lattice relaxation rate for the spin-doublet ground state of a 20-nm one-electron quantum dot as a function of the external magnetic field. Notice for all materials $1/T_1 \propto B^5$ at low-B fields. At high B the Zeeman phonon wavelength becomes smaller than the dot radius and the rate is strongly suppressed. This effect is evident at $B\sim 1$ T for the narrow gap materials, which have quite large bulk g factors. Here we assumed $E=10^4$ V/cm. The curves terminate at the level crossing, when the rate is extremely enhanced because the transition states have the same spin.

$$\mathcal{U}^{q\alpha}_{\text{e-ph}} = \sqrt{\frac{\hbar}{2\rho V \omega_{q\alpha}}} e^{i(\mathbf{q}\cdot\mathbf{r}-\omega_{q\alpha}t)} eA_{q\alpha} b^{\dagger}_{q\alpha} + \text{H.c.}, \quad (20)$$

couples these states in the presence of spin-orbit admixture. Here $b^{\dagger}_{q\alpha}$ creates an acoustic phonon with wave vector $\mathbf{q}$ and polarization $\hat{\mathbf{e}}_\alpha$ ($\alpha=L,T_1,T_2$), ρ is the material density, and V the volume of the sample. $A_{q\alpha}$ is the amplitude of the electric field created by the phonon strain, which is given by $\hat{q}_i\hat{q}_k e\beta_{ijk} e^j_{q\alpha}$, with $\hat{q}=\mathbf{q}/q$, $e\beta_{ijk}=eh_{14}$ (see Table I) for $i\neq k$, $i\neq j$, and $j\neq k$. The polarization directions are

$$\hat{\mathbf{e}}_{\text{L}} = (\sin\theta\cos\phi, \sin\theta\sin\phi, \cos\theta), \quad (21)$$

$$\hat{\mathbf{e}}_{\text{T1}} = (\cos\theta\cos\phi, \cos\theta\sin\phi, -\sin\theta), \quad (22)$$

$$\hat{\mathbf{e}}_{\text{T2}} = (-\sin\phi, \cos\phi, 0). \quad (23)$$

The transition rate is given by Fermi's golden rule,

$$\frac{1}{T_1} = \frac{V}{(2\pi)^2\hbar} \sum_\alpha \int d^3q |\langle 1|\mathcal{U}^{q\alpha}_{\text{e-ph}}|2\rangle|^2 \delta(\hbar\omega_{q\alpha} - E_2 + E_1), \quad (24)$$

which under the same perturbative approximation as Eq. (19) leads to

$$\frac{1}{T_1} \approx \frac{4}{105\pi}\left(\frac{1}{s_T^5} + \frac{3}{4}\frac{1}{s_L^5}\right)\frac{4m^{*4}(eh_{14})^2}{\rho\hbar^7}(0.61\gamma_c^2\kappa^4 + \alpha_R^2 e^2 E^2) \times \left(\frac{g_0\mu_B B}{\hbar}\right)^5 l_0^8 (n_{ph}+1)[1+\mathcal{O}(\omega_c/\omega_0)^2]. \quad (25)$$

Here s_T and s_L are the transverse and longitudinal acoustic phonon velocities, respectively. The spin-flip rate is extremely sensitive to QD radius and external magnetic field. At temperatures lower than Zeeman splitting, the emitted phonon occupation number n_{ph} is much smaller than 1, and Eq. (25) is independent of temperature. At higher temperatures Raman processes will dominate.[12]

It is interesting to study deviations from the perturbative approximation Eq. (25). In particular, at high magnetic fields the resonant phonon wavelength $\lambda_Z = hs/E_Z$ becomes much smaller than the dot radius making the dipolar approximation on the electron-phonon interaction inappropriate [Eq. (25) assumes the exponent in Eq. (20) can be approximated by $\sim 1 + i\mathbf{q}\cdot\mathbf{r}$]. Furthermore, one immediately sees that $1/T_1$ is extremely sensitive to the energy difference $E_1 - E_2$, assumed equal to the bulk Zeeman energy in Eq. (25). Here we show calculations of Eq. (24) using energy levels and eigenstates obtained by exact diagonalization in a 90 dimensional Fock-Darwin basis. In addition, we go beyond the dipolar approximation by using the identity

$$e^{i\mathbf{q}\cdot\mathbf{r}} = e^{-|\eta|^2} e^{i\eta^* a_+^\dagger} e^{i\eta a_+} e^{i\eta a_-^\dagger} e^{i\eta^* a_-}, \quad (26)$$

where $\eta(\theta,\phi) = q\ell\sin\theta e^{i\phi}/2$ depends on the polar angles of the phonon wave vector $\mathbf{q}$ [because of this dependency, we have to perform the angular integrals in Eq. (24) numerically]. Each of the exponents in Eq. (26) is expanded in powers of η, but we note that within our subspace $n_\pm \leqslant 8$, therefore only up to the ninth power needs to be retained. We checked the convergence of our calculations by reducing the Fock-Darwin subspace and noting that no appreciable change takes place for $n_+ + n_- \geqslant 4$. Our results agree with perturbation theory [Eq. (25)] at low B and E. Figure 5 shows the spin-flip rate as a function of the magnetic field. It is evident that materials such as InAs and InSb deviate from perturbation theory by more than three orders of magnitude when B is as low as 1 T. This happens because taking into account the full electron-phonon Hamiltonian leads to an exponential decrease in the rate when $q\ell \gg 1$, since Eq. (20) oscillates appreciably in this regime. Note, however, that $1/T_1 \propto B^5$ at low enough B for all materials. Figure 6 shows the dependency of the spin-flip rate with lateral confinement radius l_0 in a GaAs QD. As the electric field increases, the dependency with l_0 displays a striking behavior, which hap-

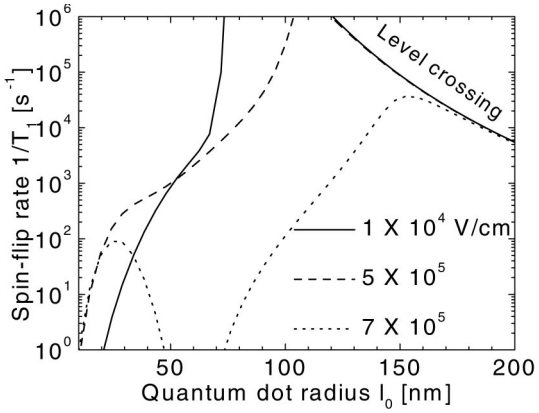

FIG. 6. Spin-flip rate $1/T_1$ due to spin-orbit admixture as a function of dot radius in GaAs. For small radius, $1/T_1 \propto l_0^8$. For $E=7\times10^5$ V/cm there is a striking change in behavior. This happens due to the sign change in g factor seen in Fig. 1.

pens due to the sign change of g factor shown in Fig. 1. A small Zeeman energy implies negligible phonon density of states, and hence the rate is zero for $l_0 \sim 50$ nm and $E=7\times10^5$ V/cm in Fig. 6. We expect $1/T_1$ will behave similarly as in Fig. 6 when g changes sign due to barrier penetration in AlGaAs,[13] this property being extremely useful in the initialization and decoherence suppression of a QD quantum computer.

We now discuss possible corrections to the simple model discussed here. At strong confinement in the 100 direction one expects Γ-X valley mixing to become important. For GaAs, $E_{\Gamma X}=0.48$ eV, which is comparable to E_{0z} [Eq. (6)] only when the electric field is the highest considered here, $E>10^6$ V/cm. This also holds true for InAs and InSb, but in GaSb Γ-X coupling will be important for $E>5\times10^5$ V/cm. Therefore even though a full $\mathbf{k}\cdot\mathbf{p}$ calculation would yield some corrections,[23] we do not expect it to change our results qualitatively in the range considered here. The same holds true for the inadequacy of the Rashba Hamiltonian, which starts deviating from Eq. (11) when $E \sim 10^6$ V/cm.[8]

Before concluding, we discuss the approximations and the limitations of this work. The most essential approximation of our model, the use of the $\mathbf{k}\cdot\mathbf{p}$ perturbation theory within an effective-mass approximation scheme to describe the conduction band, has been extensively used in the literature[20] and should be well valid for the problem we study. We have made two additional nonessential approximations in our theory in order to simplify our numerical computations: The triangular well approximation for the z confinement of the wave function and the parabolic well Fock-Darwin confinement approximation in the 2D xy plane. These approximations are reasonable enabling us to produce numerical results for a range of system parameters in several different semiconductor structures, which would have been difficult, if not impossible, to carry out had we used more realistic (and thereby numerically more demanding) quantum dot confinement potentials (The triangular well approximation was employed recently to derive new results regarding D'yakonov-Perel' relaxation anisotropy for conduction-electron spins confined by heterojunctions with $E \gtrsim 10^5$ V/cm).[24] Our most important qualitative result, establishing the viability of controlling the spin dynamics of III-V semiconductor quantum dots (both g factor and T_1 engineering) by using external gates to suitably manipulate the spin-orbit coupling through Dresselhaus and Rashba effects, should be completely independent of these approximations. In fact, we expect that the use of more sophisticated confinement models may actually make the gate control effects we predict somewhat stronger by pushing the required electric fields (and consequently 2D carrier densities) to somewhat lower values than our predicted 10^5 V/cm range. The main limitation of our predicted spin-orbit coupling induced gate control effect is, in fact, the rather large electric fields ($\sim 10^5$ V/cm) and the associated 2D carrier densities ($\sim 10^{12}$ cm^{-2}) that are required to produce significant gate control effects.

In conclusion, we show that quantum dot longitudinal g factor and spin-flip time T_1 can be controlled electrically even in the absence of wave-function overlap with a different material. These parameters show a striking dependence with dot radius and magnetic field when the 2DEG confinement is strong (electric field $E \sim 10^5$ V/cm). For example, the g factor changes sign and T_1 is extremely sensitive to the dot radius. The g factors for one-electron dots can be measured using transport spectroscopy.[25] We show that T_1 is drastically increased in narrow gap materials (InAs, InSb) due to deviations from the dipolar approximation in the electron-phonon interaction, suggesting these materials are promising for the fabrication of a quantum dot spin quantum computer. T_1 is found higher than 10^{-4} s under quite different circumstances (see Figs. 5 and 6) showing that small III-V one-electron quantum dots ($l_0<50$ nm) will have their low-temperature phase-coherence time T_2 dominated by nuclear induced spectral diffusion.[26] This result establishes the versatility of III-V quantum dots as units for single spin manipulation. A related finding of interest in our work is the dual importance of both Dresselhaus (i.e., the bulk inversion asymmetry inherent in Zincblende structures of III-V semiconductors) and Rashba (i.e., the real space structural inversion asymmetry present in a heterostructure due to external electric fields) spin-orbit coupling terms in semiconductor nanostructures—in particular, for GaAs and GaSb quantum dot structures investigated in this work, we typically find the bulk inversion asymmetry (i.e., Dresselhaus) effect to be quantitatively more important than the Rashba effect. The relative quantitative importance of the Dresselhaus effect in III-V nanostructures should have considerable significance not only in the g-factor engineering and the spin relaxation-time control of relevance to the spin quantum computer architecture (that we consider in this work), but also in the fabrication of the Datta-Das spintronic transistor,[5] where spin-orbit coupling is used to modulate a spin-polarized current in a field effect transistor configuration.

The authors acknowledge discussions with A. Kaminski and I. Žutić. This work was supported by ARDA, LPS, US-ONR, and NSF.

[1] S. Das Sarma, J. Fabian, X. Hu, and I. Žutić, Solid State Commun. **119**, 207 (2001).
[2] P. Recher, E.V. Sukhorukov, and D. Loss, Phys. Rev. Lett. **85**, 1962 (2000).
[3] I. Žutić, J. Fabian, and S. Das Sarma, Phys. Rev. Lett. **88**, 066603 (2002).
[4] D. Loss and D.P. DiVincenzo, Phys. Rev. A **57**, 120 (1998); G. Burkard, D. Loss, and D.P. DiVincenzo, Phys. Rev. B **59**, 2070 (1999); X. Hu and S. Das Sarma, Phys. Rev. A **61**, 062301 (2000); M. Friesen, P. Rugheimer, D.E. Savage, M.G. Lagally, D.W. van der Weide, R. Joynt, and M.A. Eriksson, Phys. Rev. B **67**, 121301 (2003).
[5] S. Datta and B. Das, Appl. Phys. Lett. **56**, 665 (1990).
[6] J. Nitta, T. Akazaki, H. Takayanagi, and T. Enoki, Phys. Rev. Lett. **78**, 1335 (1997); T. Koga, J. Nitta, T. Akazaki, and H. Takayanagi, *ibid.* **89**, 046801 (2002).
[7] Y.A. Bychkov and E.I. Rashba, J. Phys. C **17**, 6039 (1984).
[8] E.A. de Andrada e Silva, G.C. La Rocca, and F. Bassani, Phys. Rev. B **55**, 16 293 (1997); **50**, 8523 (1994).
[9] G. Dresselhaus, Phys. Rev. **100**, 580 (1955); M. D'yakonov and V.I. Perel', Sov. Phys. Solid State **13**, 3023 (1972).
[10] S. Tarucha, D.G. Austing, T. Honda, R.J. van der Hage, and L.P. Kouwenhoven, Phys. Rev. Lett. **77**, 3613 (1996).
[11] L. Jacak, A. Wójs, and P. Hawrylak, *Quantum Dots* (Springer-Verlag, Berlin, 1998).
[12] A.V. Khaetskii and Yu.V. Nazarov, Phys. Rev. B **64**, 125316 (2001).
[13] G. Salis, Y. Kato, K. Ensslin, D.C. Driscoll, A.C. Gossard, and D.D. Awschalom, Nature (London) **414**, 619 (2001); Y. Kato, R.C. Myers, D.C. Driscoll, A.C. Gossard, J. Levy, and D.D. Awschalom, Science **299**, 1201 (2003).
[14] H.W. Jiang and E. Yablonovitch, Phys. Rev. B **64**, 041307 (2001).
[15] L.M. Woods, T.L. Reinecke, and Y. Lyanda-Geller, Phys. Rev. B **66**, 161318 (2002).
[16] R. Vrijen, E. Yablonovitch, K. Wang, H.W. Jiang, A. Balandin, V. Roychowdhury, T. Mor, and D. DiVincenzo, Phys. Rev. A **62**, 012306 (2000).
[17] M.I. D'yakonov and V.Yu. Kachorovskii, Sov. Phys. Semicond. **20**, 110 (1986).
[18] J. Schliemann, J.C. Egues, and D. Loss, Phys. Rev. Lett. **90**, 146801 (2003).
[19] J.B. Miller, D.M. Zumbuhl, C.M. Marcus, Y.B. Lyanda-Geller, D. Goldhaber-Gordon, K. Campman, and A.C. Gossard, Phys. Rev. Lett. **90**, 076807 (2003).
[20] G. Lommer, F. Malcher, and U. Rössler, Phys. Rev. B **32**, 6965 (1985); Superlattices Microstruct. **2**, 273 (1986); E.L. Ivchenko, A.A. Kiselev, and M. Willander, Solid State Commun. **102**, 375 (1997).
[21] Z. Wilamowski, W. Jantsch, H. Malissa, and U. Rössler, Phys. Rev. B **66**, 195315 (2002); Z. Wilamowski, W. Jantsch, N. Sandersfeld, M. Muhlberger, F. Schaffler, and S. Lyon, Physica E (Amsterdam) **16**, 111 (2003).
[22] M. Cardona, N.E. Christensen, and G. Fasol, Phys. Rev. B **38**, 1806 (1988).
[23] A.A. Kiselev, E.L. Ivchenko, and U. Rössler, Phys. Rev. B **58**, 16 353 (1998).
[24] N.S. Averkiev, L.E. Golub, and M. Willander, Semiconductors **36**, 91 (2002).
[25] R. Hanson, B. Witkamp, L.M.K. Vandersypen, L.H.W. van Beveren, J.M. Elzerman, and L.P. Kouwenhoven, cond-mat/0303139 (unpublished).
[26] R. de Sousa and S. Das Sarma, Phys. Rev. B **67**, 033301 (2003); *ibid.* **68**, 115322 (2003).